NOTES AND CORRESPONDENCE

On the Accuracy of the Simple Ocean Data Assimilation Analysis for Estimating Heat Budgets of the Near-Surface Arabian Sea and Bay of Bengal*

S. S. C. SHENOI, D. SHANKAR, AND S. R. SHETYE

National Institute of Oceanography, Goa, India

ABSTRACT

The accuracy of data from the Simple Ocean Data Assimilation (SODA) model for estimating the heat budget of the upper ocean is tested in the Arabian Sea and the Bay of Bengal. SODA is able to reproduce the changes in heat content when they are forced more by the winds, as in wind-forced mixing, upwelling, and advection, but not when they are forced exclusively by surface heat fluxes, as in the warming before the summer monsoon.

1. Introduction

The interannual variability of the heat budget of the upper ocean (say, top 50 m) is of paramount interest owing to its importance for air–sea coupling. In the past, such estimates were not possible because climatologies like those of Levitus and Boyer (1994, LB hereinafter) were the only source of information on subsurface temperature on a basinwide scale. Of late, however, assimilation of data into ocean models has made available three-dimensional global fields of velocity, temperature, and salinity spanning several decades, making feasible an estimate of the interannual variability of the heat budget of the upper ocean. Among the ocean data assimilation analyses available today is that from the Simple Ocean Data Assimilation (SODA) model (hereinafter referred to as simply SODA) (Carton et al. 2000), which assimilates all available temperature and salinity observations in the world oceans, satellite altimetry, and sea surface temperature (SST) observations to constrain a numerical model of the primitive equations of motion. SODA, which has the additional advantage of being readily available to the users as a "product," has been used for studying the

heat budgets of the Atlantic and Pacific Oceans (Wang and Carton 2002) and coupled dynamics in the Indian Ocean (Xie et al. 2002). We test the suitability of SODA data for estimating the heat budget of the upper ocean for the two parts of the north Indian Ocean: the Arabian Sea and the Bay of Bengal. These basins are selected because (i) they exhibit a large seasonal and interannual signal owing to the monsoons and (ii) a balanced heat budget is already available for these two basins (Shenoi et al. 2002, hereinafter SSS).

SSS used monthly climatologies of observations to quantify the climatological heat budget of the top 50 m of the two basins. The principal objective of this exercise was to determine the factors that make the bay warmer. The shallow control volume for each basin was bounded on three sides by land and by an open southern boundary at 6°N (Fig. 1). Exchange of heat between the control volumes and their respective surroundings was possible across the air–sea interface, across the open southern boundary, and through the bottom. The monthly climatology of Josey et al. (1996) was used to estimate the fluxes across the air–sea interface, and the monthly temperature climatology of LB was used to estimate the rate of change of heat within a control volume and the diffusion of heat through its bottom. Advection of heat was estimated using the climatology of LB together with the monthly climatology of wind stress (Josey et al. 1996; used to estimate the Ekman component of the current), and that of the sea level anomalies from the Ocean Topography Experiment (TOPEX)/Poseidon (used to estimate the geostrophic component of the current). Despite these datasets being independent of one another, SSS obtained a bal-

Corresponding author address: S. S. C. Shenoi, Physical Oceanography Division, National Institute of Oceanography, Dona Paula, Goa 403004, India.
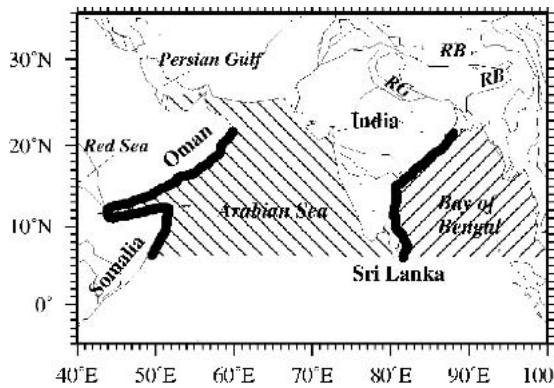E-mail: shenoi@darya.nio.org

FIG. 1. The hatched areas show the two control volumes used for estimating the heat budgets of the near-surface Arabian Sea and Bay of Bengal by SSS; the southern boundary is fixed at 6°N, which roughly marks the southern tip of Sri Lanka, and the other three boundaries are surrounded by land. The dark strips along the western boundary of the basins represent the coastal strips used by SSS for computing the contribution of coastal pumping to the heat budget. The same control volumes are used in this note to estimate the heat budget using SODA data.

anced heat budget for the two basins (see Fig. 3, bottom panel; adapted from Fig. 8 in SSS). Given appropriate datasets, the approach used by SSS can be extended to estimate the interannual variability in the heat budgets for the north Indian Ocean. This is of significance for the air–sea coupling associated with the Indian monsoon: SST in the Arabian Sea is now being used even in the statistical forecast models of the India Meteorological Department (Sen 2003; Rajeevan et al. 2004).

Of the datasets used by SSS, the sea level from TOPEX/Poseidon fulfills the requirement of a dataset that can be used for interannual variability studies, and adequate substitutes are available for the wind stress data of Josey et al. (1996). For air–sea fluxes and temperature profiles, however, the only available data sources are model reanalyses. Flux data are available from, for example, the National Centers for Environmental Prediction (NCEP)–National Center for Atmospheric Research (NCAR) reanalyses (Kalnay et al. 1996), and data on temperature are available from SODA (Carton et al. 2000).

SODA reproduces the seasonal cycle of variability in the Indian Ocean (Xie et al. 2002), and its average temperature in the top 50 m of the Arabian Sea and Bay of Bengal is within 0.5°C of that in LB (Fig. 2). The purpose of this note is to examine if SODA can serve as an adequate replacement for the datasets used by SSS for estimating the heat budget of the top 50 m of the Arabian Sea and the Bay of Bengal. An essential prerequisite for this is that it should be possible to use its climatology to balance the budget as done by SSS.

2. The heat budget

SODA uses an ocean general circulation model to interpolate unevenly distributed ocean measurements into three-dimensional global fields of temperature and velocities spanning the period 1950–2001. It has a resolution of $1° \times 1°$ in the midlatitudes and $1° \times 0.45°$ (longitude–latitude) in the Tropics; it has 20 vertical levels, with 15-m resolution near the surface. We construct a monthly climatology from the SODA data for the 30-yr period 1963–92 to estimate the heat flux due to advection and diffusion and to estimate the rate of change of heat in the 50-m-deep control volume for each basin. This is the period in which most of the observations (in the north Indian Ocean) that are used to make the LB climatology are concentrated; hence, this choice ensures that the SODA and LB climatologies represent the same epoch. As in SSS, the net flux of heat across the air–sea interface is estimated from the climatology of Josey et al. (1996), which is a refined version of the Comprehensive Ocean–Atmosphere Dataset (COADS); often called the Southampton Oceanographic Center Climatology, it also has a resolution of $1° \times 1°$.

SSS had defined the heat budget equation as

$$\frac{\overline{\rho}_w C_P}{A} \frac{\partial}{\partial t} \int_V T \, dV = -\frac{\overline{\rho}_w C_P}{A}$$

$$\times \left[\int_S T\mathbf{u} \cdot \mathbf{n} \, dS - \int_S \mathbf{F} \cdot \mathbf{n} \, dS \right],$$
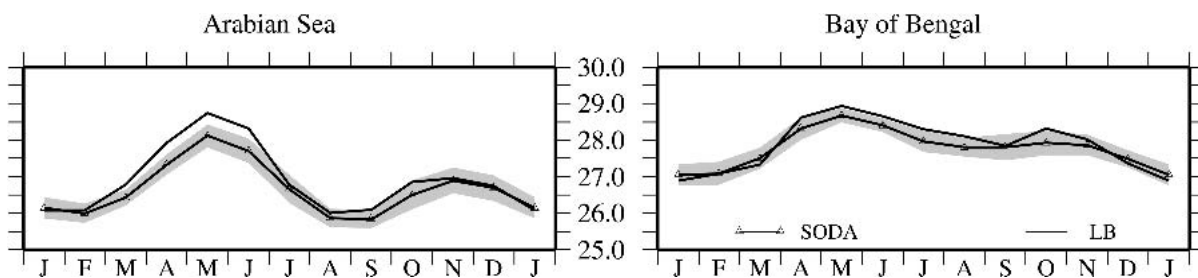
(1)

FIG. 2. Average temperature (°C) of the control volumes for the (left) Arabian Sea and (right) Bay of Bengal based on SODA climatology for 1963–92 and Levitus and Boyer (1994). The difference between the two is less than 0.5°C. The envelope (gray shade) on the curve for SODA is a measure of the interannual variability represented by one standard deviation.

where T is the temperature, $\mathbf{u}$ is the velocity, $\mathbf{F}$ represents the nonadvective fluxes, $\mathbf{n}$ is the unit vector normal to the surfaces bounding the control volume (directed outward), and the integral on the left-hand side is evaluated over the control volume; $\bar{\rho}_w = 1026$ kg m^{-3} and $C_p = 3902$ J kg^{-1}K^{-1} are the mean density and specific heat of seawater, and A is the area of the control volume at the ocean surface. The nonadvective term $\mathbf{F}$ consists of the surface fluxes and diffusion through the bottom of the control volume; diffusion through the lateral boundaries, including the open southern boundary, is negligible in comparison (SSS).

Equation (1) is used here too, but the advective term is estimated differently. Owing to the nonavailability of the vertical velocity field, SSS had split the advective process into two parts, a meridional overturning cell that exports heat out of the control volume at the southern boundary and a zonal overturning cell that arises from the cross-shore flow at the western boundary owing to coastal upwelling. The contribution of Ekman and geostrophic components of the current to each of the two advective terms (meridional overturning and zonal overturning or coastal pumping) was estimated separately. In each case, the vertical velocity field was assumed to be that required to compensate for the flux of mass into or out of the control volume. Since SODA provides a 3D velocity field, computation of the advective term is considerably simpler here.

SODA provides the horizontal and vertical velocities at different levels, together with the temperature at those levels. Therefore, the heat flux due to advection can be estimated as the sum of the heat flux across the southern boundary of the control volume (6°N) due to the meridional velocity (v) and the heat flux across the bottom of the control volume due to the vertical velocity (w). Hence, the advective term is expressed as

$$-\frac{\bar{\rho}_w C_p}{A} \int_S T\mathbf{u} \cdot \mathbf{n} \, dS = \frac{\bar{\rho}_w C_p}{A} \left(\int_x \int_z T_6 v_6 \, dz \, dx \right.$$
$$\left. + \int_x \int_y T_{50} w_{50} \, dy \, dx \right), \quad (2)$$

where T_6 and v_6 are the temperature and meridional velocity at 6°N and T_{50} and w_{50} are the temperature and vertical velocity at 50 m. The vertical integral is computed over the depth of the control volume (50 m).

The resulting heat budget is shown in Fig. 3. The rate of change of heat (q_t) in the control volume and the net fluxes (Q, atmospheric plus oceanic fluxes) are shown in the third panel from the top. The shading around the curves represents the standard deviation for each month; this is used here as an estimate of the error. The corresponding figure from SSS is shown in the bottom panel for comparison. In SSS, the budget is almost completely closed within the error limits highlighted by the shading. The curves for Q and q_t from SODA overlap within the limits defined by the standard deviations

over most of the year, February–May being the exception. Since the surface fluxes are the same as in SSS, who obtained a closed budget, this difference must stem either from the differences in q_t [the lhs of Eq. (1)], or from the differences in oceanic fluxes [advection and diffusion, i.e., the rhs of Eq. (1)], or must be due to differences in both terms. To ascertain the cause of this error, each of the terms is compared with its counterpart in SSS.

SSS used three datasets—the sea level anomalies from TOPEX/Poseidon (Le Traon et al. 1998), wind stress (Josey et al. 1996), and the monthly climatology of temperature (LB)—to estimate the advective flux. The estimate using SODA is only marginally different ($\sim$15 W m^{-2}) during September–October (Fig. 4); hence, errors in advection are unlikely to be the cause of the nonclosure of the budget during February–May (Fig. 3).

Diffusive heat flux at the bottom of the control volume depends on the vertical gradient of temperature; this is included in the second term on the rhs of Eq. (1). As in SSS, a constant diffusive coefficient ($k = 2.0 \times 10^{-4}$ m^2 s^{-1}) has been used (Zhang and Talley 1998) in the absence of the variable, Richardson-number-dependent coefficients that were used internally in the model; this, however, is acceptable because the model diffusion field is not available to users as part of the SODA product. Except during October–November, the differences between the diffusive fluxes in SODA and SSS ($\sim$15 W m^{-2}) are not significant in both basins because the diffusion estimate based on LB is within the interannual variability of diffusion estimated from SODA (Fig. 4). Hence, errors in diffusion also cannot be responsible for the nonclosure of the budget during February–May (Fig. 3).

Qualitatively, the q_t estimated from SODA and LB are similar (Fig. 4), as may be expected from the similarity in the temperature (Fig. 2). The difference between the two is, however, significant when the ocean warms; this happens 2 times per year in both basins, during February–May before the summer monsoon (Sengupta et al. 2002) and during September–November after the summer monsoon. SODA almost captures the second warming, but not the first. The mismatch between q_t and Q is greater than 50 W m^{-2}, which is larger than the sum of the standard deviations of q_t and Q, during April in the Arabian Sea (Fig. 3). This error is large enough to prevent a closure of the heat budget even though the temperature error of 0.5°C is within "tolerable limits" for many other purposes. In the bay, the cooler spring temperatures in SODA extend into the summer monsoon, but the weaker diffusion (Fig. 4) permits a better closure of the budget during the summer monsoon than in spring.

This inability of SODA to close the budget during February–May is also true of other temporal subsets of the 1950–2001 period for which SODA data are available: the same problem exists during 1970–79, 1980–89,
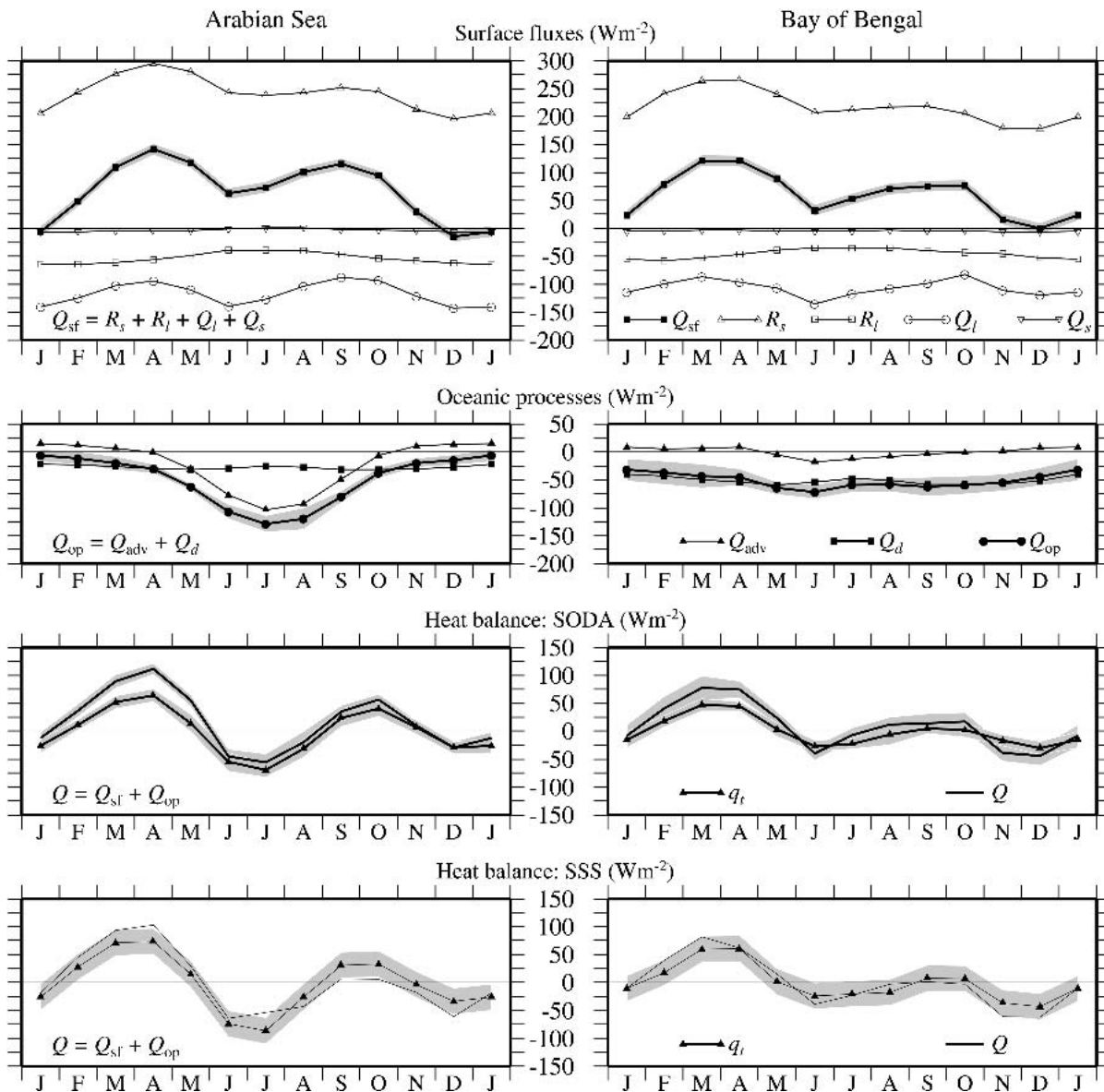
FIG. 3. The heat budget of the upper ocean in the (left) Arabian Sea and (right) Bay of Bengal. Climatological SODA temperature and velocities are used for estimating the heat budget; the SODA climatology is computed for 1963–92. (top) Climatological monthly mean net shortwave radiation (R_s), net longwave radiation (R_l), latent heat flux (Q_l), and sensible heat flux (Q_s), and their sum, the net surface flux (Q_{sf}). The envelope (gray shade) shows the presumed standard deviation of 10 W m^{-2} on Q_{sf} based on Josey et al. (1999) and Weller et al. (1999). (second from top) Fluxes due to oceanic processes Q_{op}: advection (Q_{adv}) and diffusion (Q_d); the sum of the fluxes due to these processes (Q_{op}) and the monthly standard deviation (gray shade) are also shown. (third from top) Rate of change of heat (q_t) in the control volumes and the net flux of heat ($Q = Q_{sf} + Q_{op}$) into or out of them. The envelope on the curves (gray shade) represents the standard deviation due to interannual variability. (bottom) Adapted from SSS (their Fig. 8) and similar to the third row of panels, but the curves are based on the datasets used by SSS.

1990–2001, and 1980–93, this being the period corresponding to the surface flux climatology of Josey et al. (1996). The only difference was in the standard deviation, it being higher for the earlier decades (1970–79 and 1980–89) and lower for the later decades (1990–2001). The higher standard deviation in the earlier decades is partly due to the fewer observations available then for assimilation, but another reason may be decadal variability. It is not possible, however, to separate these effects on the standard deviations of the SODA product.

Replacing the q_t from SODA with that from LB, however, balances the heat budget to the same extent as in SSS (Fig. 5). The budget now closes because of two reasons. First, the two q_ts are different. Second, the error in LB is much greater than the standard deviation,
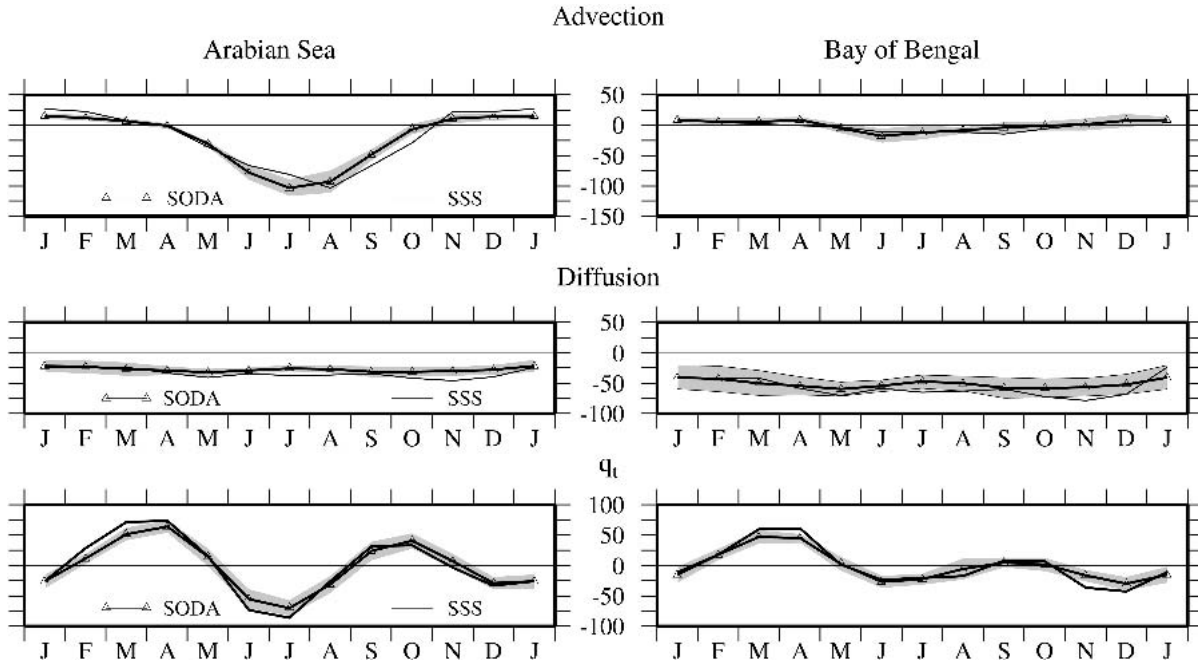
FIG. 4. Comparisons for (top) advective flux (Q_{adv}), (middle) diffusive flux (Q_d), and (bottom) the rate of change of heat in the control volumes (q_t) for the (left) Arabian Sea and (right) Bay of Bengal between SSS and this note. The shading on the curves for SODA represents one standard deviation and is a measure of the interannual variability in the SODA data.

or interannual variability, in SODA, resulting in a thicker envelope around the curve. Since the interannual variability in SODA is much less than the difference in temperature between SODA and LB, it is likely that the errors in SODA temperature are greater than the interannual variability; merely thickening the SODA error envelope in Fig. 3 (third panel from the top), however, is not sufficient to balance the budget.

3. Discussion

The suitability of SODA data for estimating the heat budget of the upper ocean has been tested for the two parts of the north Indian Ocean: the Arabian Sea and

the Bay of Bengal. Both basins exhibit a large seasonal and interannual signal owing to the monsoons, making them an ideal test of SODA's potential as a tool for studying interannual variability of the heat budget of the upper ocean. Except during February–May, the climatological heat budget computed using SODA closes to the same extent as in SSS, who used a variety of datasets for the purpose.

The average temperature in the north Indian Ocean follows a bimodal distribution: there are two maxima (during April–May and September–October) and two minima (during the summer monsoon, which peaks in July, and during winter). The cooling during the summer monsoon in the Arabian Sea is due to two causes:
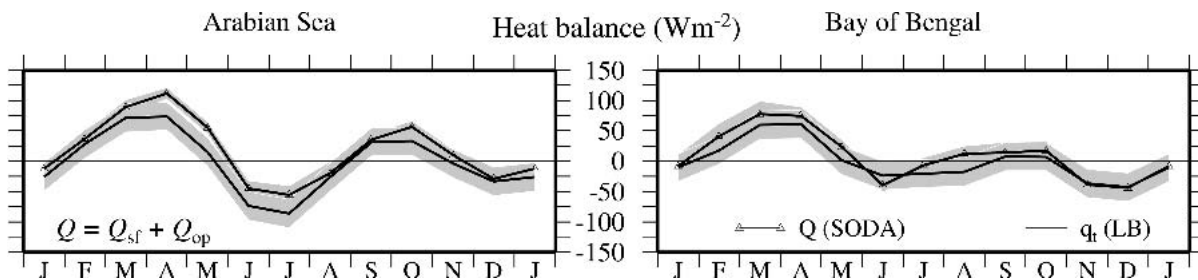
FIG. 5. The effect of replacing the q_t from SODA with that from LB. The two curves are the q_t from LB (as in the bottom panel of Fig. 3) and Q, the sum of surface fluxes from Josey et al. (1996) and oceanic processes from SODA (as in the third panel of Fig. 3). The envelope around Q is the standard deviation of the SODA Q and is representative of the interannual variability in SODA; that around q_t is due to the error in the annual mean temperature field of LB (0.3°C). Replacing the q_t from SODA with that from LB balances the heat budget to the same extent as in SSS.

to the deepening of the mixed layer owing to mixing by the strong monsoon winds and to the strong upwelling and cross-equatorial flow that take place along the western boundary (SSS). Both are directly related to the momentum flux at the surface, and therefore to the strength of the winds. The cooling that takes place during winter in the Arabian Sea is due to convective overturning (see, e.g., McCreary et al. 1993). This occurs because of the cooling of the surface of the ocean by the winds during the winter monsoon, which results in an unstable stratification and the upper ocean overturns. Thus, this second cooling during the year in the Arabian Sea is related to both momentum fluxes and surface heat fluxes. The warming that precedes and succeeds the summer monsoon cooling is exclusively due to surface heat fluxes (Sengupta et al. 2002). The surface of the ocean warms rapidly during February–May as the sun moves over the Northern Hemisphere; it also warms following the monsoon because the winds weaken and the clouds disappear, but this postmonsoon warming is much weaker than the premonsoon warming. The Bay of Bengal, as shown by SSS, is very different from the Arabian Sea. The winds over the bay are relatively weak, forcing a weaker circulation and much weaker vertical transport. Hence, the SST is higher in the bay, resulting in strong convective activity, which implies higher rainfall and a stronger stratification near the surface. The stratification, in turn, inhibits upwelling during the summer monsoon and allows SST to remain high (Vinayachandran et al. 2002). Therefore, the weaker winds over the bay decouple the dynamics from the thermodynamics of the upper ocean: the warming and cooling in the surface layers of the bay is controlled more by the surface heat fluxes.

The budget computed using SODA closes for both basins except during the spring warming (February–May), but the difference between q_t and Q, though within the tolerance limits at other times of the year, is large during the warming following the summer monsoon in the Arabian Sea, and during the summer monsoon and during the warming following it in the Bay of Bengal (Figs. 3 and 2). Thus, in the north Indian Ocean, the SODA data are able to reproduce the changes in heat content when they are forced more by the wind stress and are related to the surface momentum fluxes, but not when they are forced only by the surface heat fluxes.

REFERENCES

Carton, J., G. Chepurin, X. Cao, and B. Giese, 2000: A simple ocean data assimilation analysis of the global upper ocean 1950–95. Part I: Method. *J. Phys. Oceanogr.,* **30,** 294–309.

Josey, S., E. Kent, D. Oakley, and P. Taylor, 1996: A new global air–sea heat and momentum flux climatology. *International WOCE Newsletter,* No. 24, WOCE International Project Office, Southampton, United Kingdom, 3–5.

——, ——, and P. Taylor, 1999: New insights into the ocean heat budget closure problem from analysis of the SOC air–sea flux climatology. *J. Climate.,* **12,** 2856–2880.

Kalnay, E., and Coauthors, 1996: The NCEP/NCAR 40-Year Reanalysis Project. *Bull. Amer. Meteor. Soc.,* **77,** 437–471.

Le Traon, P. Y., F. Nadal, and N. Ducet, 1998: An improved mapping method of multi-satellite altimeter data. *J. Atmos. Oceanic Technol.,* **15,** 522–534.

Levitus, S., and T. P. Boyer, 1994: *Temperature.* Vol. 4, *World Ocean Atlas 1994,* NOAA Atlas NESDIS 4, 117 pp.

McCreary, J. P., P. K. Kundu, and R. L. Molinari, 1993: A numerical investigation of the dynamics, thermodynamics and mixed-layer processes in the Indian Ocean. *Progress in Oceanography,* Vol. 31, Pergamon, 181–244.

Rajeevan, M., D. S. Pai, S. K. Dikshit, and R. R. Kelkar, 2004: IMD's new operational models for long-range forecast of southwest monsoon rainfall over India and their verification for 2003. *Curr. Sci.,* **86,** 422–431.

Sen, N., 2003: New forecast models for Indian south-west monsoon season rainfall. *Curr. Sci.,* **84,** 1290–1292.

Sengupta, D., P. K. Ray, and G. S. Bhat, 2002: Spring warming of the eastern Arabian Sea and Bay of Bengal from buoy data. *Geophys. Res. Lett.,* **29,** 1734, doi:10.1029/2002GL015340.

Shenoi, S., D. Shankar, and S. Shetye, 2002: Differences in heat budgets of the near-surface Arabian Sea and Bay of Bengal: Implications for the summer monsoon. *J. Geophys. Res.,* **107,** 3052, doi:10.1029/2000JC000679.

Vinayachandran, P. N., V. S. N. Murty, and V. R. Babu, 2002: Observations of barrier layer formation in the Bay of Bengal during summer monsoon. *J. Geophys. Res.,* **107,** 8018, doi: 10.1029/2001JC000831.

Wang, J., and J. Carton, 2002: Seasonal heat budgets of the North Pacific and North Atlantic Oceans. *J. Phys. Oceanogr.,* **32,** 3474–3489.

Weller, R. A., M. F. Baumgartner, S. A. Josey, A. S. Fischer, and J. Kindle, 1999: Atmospheric forcing in the Arabian Sea during 1994–1995: Observations and comparisons with climatology and models. *Deep-Sea Res.,* **45B,** 1961–1999.

Xie, S., H. Annamalai, F. Schott, and J. McCreary, 2002: Structure and mechanisms of south Indian Ocean climate variability. *J. Climate.,* **15,** 867–878.

Zhang, H., and L. Talley, 1998: Heat and buoyancy budgets and mixing rates in the upper thermocline of the Indian Ocean and global oceans. *J. Phys. Oceanogr.,* **28,** 1961–1978.